View metadata, citation and similar papers at core.ac.uk

brought to you by CORE

provided by DigitalCommons@USU

Utah State University

DigitalCommons@USU

International Symposium on Hydraulic Structures

May 17th, 2:10 PM

Application of a Free-surface Immersed Boundary-lattice Boltzmann Modeling to Wave Forces Acting on a Breakwater

Badarch Ayurzana Mr
Mongolian University of Science and Technology, ayur_426@yahoo.com

Hosoyamada Tokuzo Mr
Nagaoka University of Technology, Nagaoka, rng@nagaokaut.ac.jp

Tungalagtamir Erdenebayar Mrs
Nagaoka University of Technology, tungalag401@gmail.com

Follow this and additional works at: https://digitalcommons.usu.edu/ishs

Recommended Citation

Ayurzana, Badarch (2018). Application of a Free-surface Immersed Boundary-lattice Boltzmann Modeling to Wave Forces Acting on a Breakwater. Daniel Bung, Blake Tullis, 7th IAHR International Symposium on Hydraulic Structures, Aachen, Germany, 15-18 May. doi: 10.15142/T3P92D (978-0-692-13277-7).

This Event is brought to you for free and open access by the Conferences and Events at DigitalCommons@USU. It has been accepted for inclusion in International Symposium on Hydraulic Structures by an authorized administrator of DigitalCommons@USU. For more information, please contact digitalcommons@usu.edu.

UtahStateUniversity
MERRILL-CAZIER LIBRARY

7th International Symposium on Hydraulic Structures Aachen, Germany, 15-18 May 2018
ISBN 978-0-692-13277-7 DOI: 10.15142/T3P92D

Application of a Free-Surface Immersed Boundary-Lattice Boltzmann Modeling to Wave Forces Acting on a Breakwater

B. Ayurzana[1], T. Hosoyamada[2] & E. Tungalagtamir[1]
[1]*Mongolian University of Science and Technology, Ulaanbaatar, Mongolia*
[2]*Nagaoka University of Technology, Nagaoka, Japan*
E-mail: ayur_426@yahoo.com

Abstract: *A novel free-surface immersed boundary-lattice Boltzmann method for wave–structure interaction and hydrodynamic force estimation is introduced. The free-surface lattice Boltzmann method is coupled with the immersed boundary modification in order to simulate rigorous free surface wave and to evaluate the exact hydrodynamic forces on a breakwater. First, the proposed model is applied to incident wave propagation in a shallow water zone. The wave–breakwater interactions and wave forces on a breakwater are then analysed using the method. The results agreed with those of Goda's formulae, confirming that the proposed model has a high potential for application to complex analysis of coastal engineering problems.*

Keywords: *Wave–structure interaction, wave force, immersed boundary, Lattice Boltzmann method.*

1. Introduction

The evaluation of wave forces acting on a breakwater is the main requirement for a correct analysis of breakwater stability (Goda 2010). The design methods for wave forces have been established from numerical models based on the theory or the fluid governing equations such as the Navier-Stokes equations or shallow water equations (Guanche et al., 2009; Hayakawa et al., 1998). Numerical methods based on the governing equations have been extensively studied and applied to wave–structure interactions, e.g., both the Eulerian and Lagrangian methods such as the volume of fluid (VOF) method, smoothed particle hydrodynamics (SPH), and moving particle semi-implicit method (MPS) are proposed to simulate complex waves and flow fields around breakwaters (Altomare et al., 2015). In addition, the lattice Boltzmann method (LBM) for the shallow water equation has been successfully introduced to wave propagation studies (Zhou, 2010; Koshimura and Murakami, 2009). Nevertheless, the force and pressure evolution of the LBM for shallow water systems requires further improvements.

In previous studies on coastal engineering in Japan, LBM methods were used for modeling of free surface flows (Araki and Koshimura, 2009), tsunamis (Koshimura and Murakami, 2009), multi-phase flows (Araki and Koshimura, 2010), and motion of bed loads (He et al., 2013). These studies show that the LBM method has a potential for application to complex wave fields and their extensions. There are no previous studies on using the LBM for estimation of wave pressures and forces. Thus, we propose the estimation of wave forces using the LBM with immersed boundary (IB) method. As a proposed numerical model, the free-surface lattice Boltzmann method introduced by Korner et al. (2005) is coupled with the immersed boundary modification by Noble and Torczynski (1998) in order to simulate rigorous free surface wave and to evaluate the smooth hydrodynamic forces on the caisson block.

With the increasing function of breakwaters, the role of numerical simulation is becoming more important. Currently, the LBM is a relatively new approach to coastal engineering applications that can handle wave and wave forces on coastal structures. Particularly, the lattice Boltzmann (LB) modeling for a free surface flow and fluid–solid interactions will provide an alternative and attractive solution for coastal engineering problems. In this study, we show the application of a free-surface immersed boundary-lattice Boltzmann method (FS-IB-LBM) for wave force estimation on a breakwater and wave–structure interactions. The numerical study covers the interactions between violent waves and breakwater, and the effect of overtopping waves and uplift on the forces acting on the caisson of a typical breakwater. The evaluation of the wave forces acting on the breakwater is performed and discussed thoroughly.

2. Numerical Models

Recently, LB modeling is being extended into many areas involving physics and chemistry as well as engineering and industry. As being braided, the types of LB modeling have emerged as versions to be differentiated from the original concept of LBM (Aidun and Clausen, 2010). In this study, we use one of the original procedures of LB modeling for a fluid flow, called D2Q9 lattice, with the Bhatnagar-Gross-Krook (BGK) collision operator (Chen and Doolen, 1998). With regard to this, the existing LB models with specific modifications are introduced and proposed as the numerical model, called FS-IB-LBM, for the wave–structure interactions.

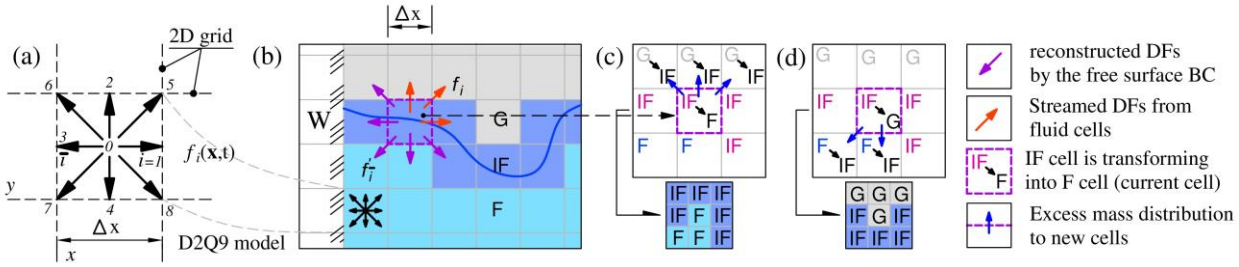

Figure 1. Some descriptions of free surface lattice Boltzmann method: (a) lattice arrangement in a cell, (b) cell types and distribution functions for free surface boundary condition, and (c) - (d) possible transformation of IF cells and neighbouring cells. DFs – distribution functions and BC – boundary condition.

2.1. Free-Surface Lattice Boltzmann Modeling

From the widely recognized two types of free surface flow modeling in LB modeling, namely single-phase and multi-phase modeling, the simple single-phase modeling introduced by Korner et al. (2005) is adopted for the proposed model. The free surface model is formulated using the concept of the VOF method in terms of the mesoscopic way, which is the basic description scale of LB modeling (Aidun and Clausen, 2010). In the free-surface LBM, each cell has a volume fraction value of fluid that is expressed as the ratio of the mass to the density of the cell: m/ρ. Depending on the volume fraction value of fluid, each cell is marked by flags (Araki and Koshimura, 2010; Badarch et al., 2016) as an indication of the materials in the computational cells, such are F for fluids (water), G for gases (air), W for solids, and IF for interface cells, as shown in Fig. 1(b).

Because of its advantage of being a single-phase model, the discretized Boltzmann equation:

$$f_i(\boldsymbol{x} + \boldsymbol{c}_i\delta t, t + \delta t) - f_i(\boldsymbol{x}, t) = \Omega_i \tag{1}$$

is numerically considered for only the liquid cells, which are the F and IF cells. In Eq. (1) with Fig. 1(a), $f_i(\mathbf{x}, t)$ is the density distribution function (DF) at position **x** and time *t* discretized from the one-particle DF in a phase space (Chen and Doolen 1998) and Ω_i is the collision operator altered by the BGK collision operator (Aidun and Clausen 2010) with the external force term (Badarch et al 2016):

$$\Omega_i = -\delta t \frac{f_i(x,t) - f_i^{eq}(x,t)}{\tau_{tot}} + \delta t F_i \,, \tag{2}$$

where τ_{tot} is the total relaxation time with respect to the total viscosity that can be defined by the Smagorisky turbulent model (Hou et al., 1996; Chen and Doolen, 1998). In Eq. (2), f_i^{eq} is the equilibrium DF approximated from the Maxwell distribution (Aidun and Clausen, 2010) for incompressible flow:

$$f_i^{eq} = w_i\rho\left[1 + \frac{\boldsymbol{u}\boldsymbol{c}_i}{c_s^2} - \frac{\boldsymbol{u}^2}{2c_s^2} + \frac{\boldsymbol{u}^2\boldsymbol{c}_i^2}{2c_s^4}\right], \tag{3}$$

and F_i is the force term (Badarch et al., 2016) as

$$F_i = w_i\left(1 - \frac{1}{2\tau_{tot}}\right)\left[\frac{\boldsymbol{c}_i - \boldsymbol{u}}{c_s^2} + \frac{\boldsymbol{c}_i(\boldsymbol{c}_i\boldsymbol{u})}{c_s^4}\right] \cdot \boldsymbol{F} \,. \tag{4}$$

The basic macroscopic fluid variables, density ρ, velocity **u**, and pressure p, are defined from the DFs as

$$\rho = \sum_{i=0}^{8} f_i \ , \quad \rho \boldsymbol{u} = \sum_{i=0}^{8} \boldsymbol{c}_i f_i + \frac{\boldsymbol{F}\delta t}{2} \ and, p = c_s^2 \rho \ , \tag{5}$$

where **F** is the dimensionless force density, i.e., **F** = ρ**g**, and **g** is the acceleration due to gravity; c_s is the speed of sound in the lattice form. The multi–scale expansion from the discretized Boltzmann equation in Eq. (1) retrieves the dimensionless Navier-Stokes equations in a low Mach number flow (Aidun and Clausen, 2010). This is the main evidence that LB models are promising techniques to solve fluid flows (Chen and Doolen, 1998), and this has been confirmed by many validation works during all stages of their development.

The free surface is represented as chained single-layer interface cells having an arbitrary volume fraction value of 0 to 1, and the evolution of the free surface is tracked by the mass calculation of interface cells and cells other than solid and gas cells, which have no water fraction content nor the computation of the DFs. The mass calculation on an IF cell is defined by an equation derived from the mesoscopic discretization (Korner et al., 2005) of the mass conservation equation (Christian and Krafczyk, 2011) in the VOF model:

$$m(\boldsymbol{x}, t + \delta t) = m(\boldsymbol{x}, t) + \sum_{i=0}^{8} \Delta m_i(\boldsymbol{x}, t + \delta t) \ , \tag{6}$$

where Δm_i is the mass flux value between the IF and F cells. The value of the mass on an IF cell, which in turn is the volume fraction value that defines the IF cell, is either filled or emptied. Based on the filled or emptied situation, the transformation of the free surface (IF cells) are decided as explained in Fig. 1 (b, c, and d). For instance, if an IF cell is filled, it is going to become an F cell in next time step. This change of flag also changes the neighboring cell status as G to IF and F to G, as shown in Fig. 1(c). After these changes of flags or status, the excess mass of the IF cell that was filled (or emptied for the other case) is distributed to the newly generated IF cells. The boundary condition (BC) for the free surface is defined by the detailed flux conservation equation (Korner et al., 2005) of the DFs on the IF cell:

$$f_{\bar{\imath}}'(\boldsymbol{x}, t + \delta t) = f_i^{eq}(\rho_A, \boldsymbol{u}) + f_{\bar{\imath}}^{eq}(\rho_A, \boldsymbol{u}) - f_i(\boldsymbol{x}, t) \ , \tag{7}$$

where $\bar{\imath}$ is the direction index opposite to i, as shown in Fig. 1(b), and ρ_A is the air density, which is directly related to the air pressure by the equation of state in lattice form.

The bounce-back scheme is imposed on the solid surface recognized as a non-immersed body to express a rough surface. For simulations, immersed bodies can be movable, and the IB method is employed. If the water is at rest and the depth of water is considerable, the hydrostatic pressure must be given for the initial condition to balance the force field. This initial condition can be expressed in terms of density derived from the barometric formula using $c_s = 1/\sqrt{3}$ and $\rho_0 = 3P_0$:

$$\rho(z) = \rho_0 e^{3gz} \ , \tag{8}$$

where z is the depth of water in initial state and P_0 is the reference pressure at the free surface. The additional details of the free surface LBM and its implementation can be found in the references (Araki and Koshimura, 2009; Christian and Krafczyk, 2011; Badarch 2017).

2.2. Immersed Boundary Method

The IB-LBM is reported to be a more consistent and smoother method for the force estimation compared to the native force estimation scheme in LBM known as the momentum exchange method (Feng and Michaelides, 2004). Because the IB method is introduced to the grid-based numerical methods, the previous difficulties encountered when handling movement of or complicated shapes of a body are eliminated, and the BC is formulated in the governing equations as a force term due to the IB (Strack and Cook, 2007). Superior to conventional methods, the LBM is known as the simplest method for flows around complicated geometries as well as in flows with moving immersed boundaries (Feng and Michaelides, 2004). Noble and Torczynski successfully introduced the IB modification into Eq. (1) that allows for large numbers of nonconforming, evolving boundaries but retains the advantage of the LBM (Noble and Torczynski, 1998). The IB method modifies the collision term in Eq. (2) as

$$\Omega_i = -\frac{\delta t(1-\beta)}{\tau_{tot}}\left(f_i(\boldsymbol{x},t) - f_i^{eq}(\boldsymbol{x},t)\right) + \beta f_i^m(\boldsymbol{x},t) + \delta t F_i\,, \tag{9}$$

where β is the weighting function of the solid fraction, s_f, and is defined as

$$\beta\left(s_f, \tau_{tot}\right) = \frac{s_f(\tau_{tot}-0.5)}{(1-s_f)+(\tau_{tot}-0.5)}\,, \tag{10}$$

where s_f takes a value of 0 and 1 at its limits representing the fluid and solid, respectively, as shown in Fig. 2. The additional term (Noble and Torczynski, 1998), f_i^m, in Eq. (9) is based on the bounce-back rule concept of the non-equilibrium part of the DF and is given by

$$f_i^m(\boldsymbol{x},t) = f_{\bar{i}}(\boldsymbol{x},t) - f_i(\boldsymbol{x},t) + f_{\bar{i}}^{eq}(\rho,\boldsymbol{u}_s) - f_i^{eq}(\rho,\boldsymbol{u})\,, \tag{11}$$

where $\mathbf{u}_s$ is the velocity of the solid, which is zero for stationary objects. If the cell is fluid ($s_f = 0$), the weighting function of the solid fraction becomes zero, and the discretized Boltzmann equation has no effect on the additional term in Eq. (9). Otherwise, in the limit of the solid, the weighting function of the solid fraction cancels the BGK collision in Eq. (9), and f_i in Eq. (1) cancels with $f_{\bar{i}}$ in Eq. (11). The remaining combination, $f_{\bar{i}}^{eq}(\rho,\mathbf{u}_s) - f_i^{eq}(\rho,\mathbf{u})$ accounts for the solid response to the bounce–back condition. The verification and extension of this method to a 3D model can be found in (Strack and Cook, 2007) and many other references (Feng and Michaelides, 2004).

2.3. Computation of Wave Forces

The LBM has several options to estimate the hydrodynamic force on a solid surface (Chen and Doolen, 1998). In this study, we will consider three approaches for the wave forces on the breakwater, namely the IB method, pressure integration (PI) method, and Goda's formula (GF). The latter one is used to validate the proposed FS-IB-LBM.

We modified the original formula of Noble and Torczynski (1998) for the hydrodynamic force estimation by considering the submerged parts of the immersed body (Ayurzana and Hosoyamada, 2018) in the free surface flow:

$$\boldsymbol{F}_f = s\frac{\Delta x^2}{\Delta t}\sum_n \beta_n \sum_{i=0}^{8} f_i^m \boldsymbol{c}_i\,, \tag{12}$$

where $\mathbf{F}_f$ is the force per unit length, n is the number of cells partially or fully covered by solid, and the submerged volumetric percent, s, is shown in Fig. 2 as the hatched area in the caisson.

With known wave parameters, Goda formulated the pressure formulae for the loads on coastal structures (Goda, 2010). When the wave pressures depicted in Fig. 2 are known, the wave forces can be computed by

$$\begin{aligned} F_x &= \frac{1}{2}\{(p_1+p_3)h' + (p_1+p_4)h_c\} \\ F_y &= \frac{1}{2}p_v B \end{aligned}\,. \tag{13}$$

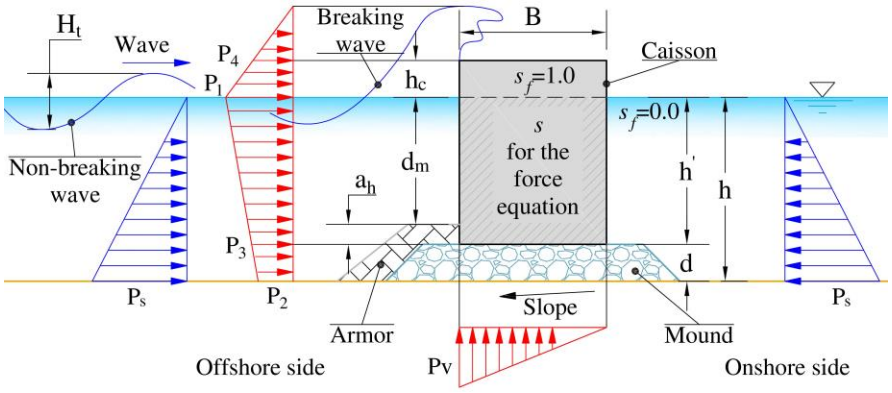

Figure 2. Schematic of Goda's pressure distribution in a typical breakwater.

2.4. Implementation of the Proposed Model

Implementation of the FS-IB-LBM is straightforward from the implementation of streaming–collision fashion for the standard LBM. For a turbulent free surface flow and to attain stability of numerical simulations, the sub-grid scale model is employed. The model can also adopt other advanced techniques for turbulent flows such as entropic treatment (Dorschner et al., 2017) and cascaded or central moment scheme for collision operator (De Rosis and Leveque, 2016). In these cases, models need to be implemented in parallel as same as described in Ayurzana et al. (2017) to be effective in terms of computational cost. Except the free surface algorithm, the parallelization of the FS-IB-LBM is direct for the local IB treatment.

In the FS-IB-LBM, the free surface algorithm requires special care for the cell type transformation, i.e., the free surface transformation. On the other hand, the IB modification is embedded in the collision steps, and the force estimation in the LBM can be defined after the macroscopic variables are computed. If the motion of the immersed body induced by the fluid flow is present, the equation of motion needs to be implemented. In this paper, the objective of the study and the fixed breakwater justify the exclusion of the equation of motion. However, it should be noted that the FS-IB-LBM can be extended to the stability analysis of breakwater considering the effects, for instance, of the appropriate value of friction between the mound and vertical breakwater. Another feature of the IB method is the probabilistic solution for the porous media flow with an advanced algorithm. The IB solution provides a potential result when applying the partial bounce-back method designed for porous media flow. The rubble mound under the caisson is assumed as a porous media having a porosity of 0.45, and the flow through the mound has been considered in the proposed model.

3. Application to Wave Forces Acting on a Breakwater

First, the model case without a breakwater was investigated to determine the wave parameters for GF. With the same condition and setup, a breakwater is placed and the prescribed force computation and wave–structure interactions are studied. The details of the simulation are given in the following sections.

3.1. Incident Wave Propagation

The geometry of the computational domain is shown in Fig. 2 and is formed with 200 m in length and 52 m in height. The grid spacing was chosen as $\Delta x = 0.25$ m and the associated time step as $\Delta t = 7.57 \times 10^{-4}$ s. For the wave propagation simulation, the breakwater and its mound were removed from the domain. To generate the wave, the velocity boundary condition (Zou and He 1997) was imposed with the shallow water approximation,

$$u = \frac{H_t}{2}\sqrt{\frac{g}{h}}\,sin\left(\frac{2\pi}{T}\right), \tag{14}$$

in the depth, *h*, and the wave period of 10 s. As the wave is passing through the outlet boundary, the zero gradient boundary condition (Jansen and Krafczyk, 2011) was employed. The total simulation time was set as 92 s for all simulations.

The wave generated by the proposed model with the given boundary condition resulted in a shallow water wave with a maximum height of $H_t = 10$ m, period of 10 s, and wavelength of 137.5 m. The general shape of the crests was a breaking wave and troughs were gentle. The crest propagates to the right about a maximum velocity of 15 m/s and passes through the outlet boundary with a slight loss of kinetic energy, which is shown by the non-breaking wave crest near the outlet boundary. The wave velocity decreases in depth, which is a characteristic of a gravity wave. In Fig. 3, the progressive waves at four specific times are shown with the velocity magnitudes. The created streamline patterns as depicted in Fig. 3 show the exact feature of surface gravity waves as the streamlines are in the direction of wave propagation at all depths below the crests, and the opposite direction at all depths below the troughs.

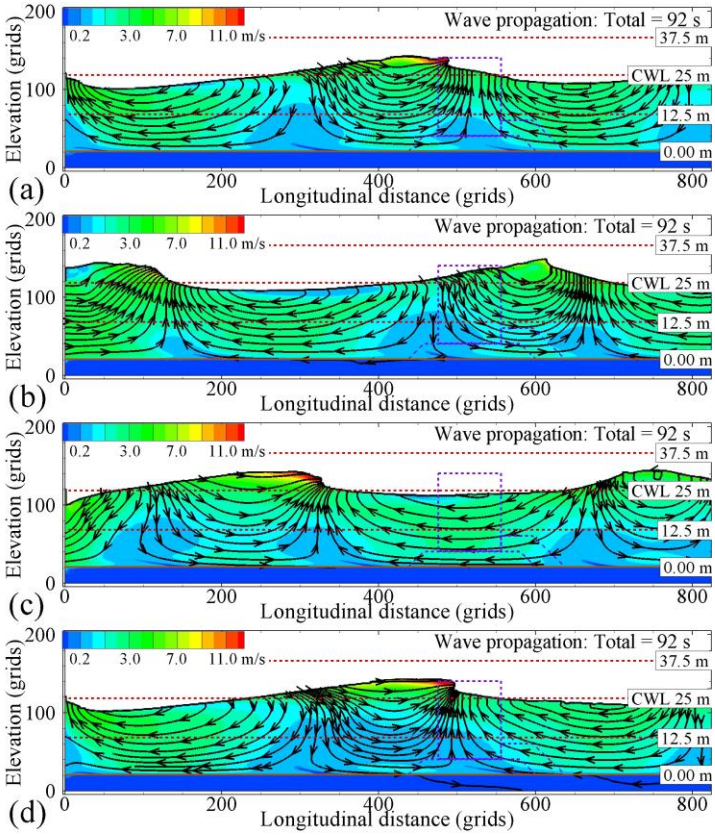

Figure 3. Instantaneous streamline patterns in a shallow water wave generated by the proposed model at (a) 30 s, (b) 33 s, (c) 37 s, and (d) 40 s after the simulation started.

The water surfaces at two points, spaced 2 m from the caisson in the offshore side and onshore side, are supposed to be measured during the simulation in order to examine the performance of the breakwater. The time series of the water surfaces with and without the breakwater are shown in Fig. 4. The waves without breakwater (NoB in Fig. 4) are the results of wave propagation, whereas the waves with a breakwater (B in Fig. 4) are measured from the simulation with a breakwater. The discrepancy between water surface elevations in progressive waves (solid red and dashed blue lines of NoB) is observed in Fig. 4. Two reasons for the discrepancy can be attributed to the following: (1) the distance between two measurement points was 24 m, and (2) the small amount of reflection on the outlet boundary was generated owing to the zero–gradient boundary condition. The wave reflection on the outlet boundary condition requires further exploration.

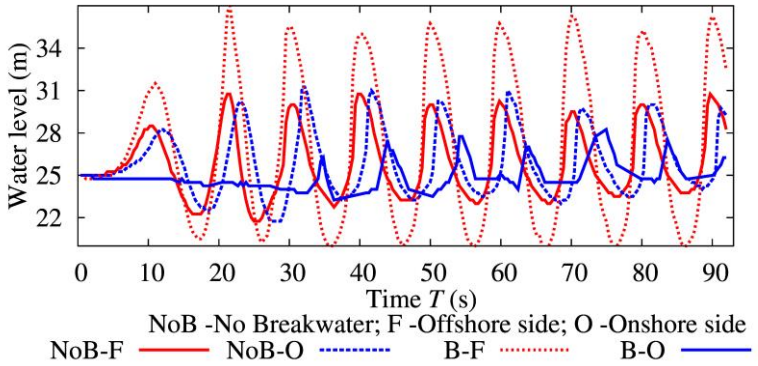

Figure 4. Free surface records from the simulations with (B) and without (NoB) breakwater.

3.2. Wave Forces Acting on a Breakwater

The breakwater without armor block is considered for the simulation. The height of the breakwater including the mount is 30 m and the normal water level (NWL) is set as 25 m in both sides of the breakwater. A wave is generated with the same condition applied in the simulation of incident wave propagation. As shown in Fig. 4, the water surface variations in both sides of the breakwater are measured and plotted as B-F and B-O, offshore side, and onshore side, respectively. The water surface with the breakwater in the offshore side increased in height because of the wave reflection on the caisson wall, as shown in Fig. 4. The wave reflected on the caisson wall traveled and collided with the incoming successive wave and made a crest with high amplitude near the caisson wall. This wave crest with high amplitude plunged on the caisson wall and further flowed over into the onshore side of the breakwater. The wave reflection coefficient was calculated to be between 0.76 and 1.0 in the given conditions. The wave in the onshore side had disappeared, and the water surface was simultaneously decreased until the third wave. The third wave and other waves progressively flowed over the caisson wall as overtopping flow, and the wave was transmitted to the onshore side, as shown by the solid blue lines in Fig. 4. The wave is not only transmitted by the overtopping flow but also transmitted by the seepage flow under the caisson wall. The seepage flow is calculated by the IB method, as shown in Fig. 5. The wave–breakwater interactions at specific times are plotted with the velocity magnitude and vector in Fig. 5. The wave run-up to the caisson wall is shown in Fig. 5(a) and (b), while the over flowing event is shown in Fig. 5(b). A wave reflected on the caisson wall is plunging with an approaching wave in offshore side in Fig. 5(c). Although the reflected wave produces high amplitudes in the crest after plunging, the energy of the approaching wave is considerably dissipated by the plunge and then the wave hits the caisson wall.

The hydrodynamic forces on the breakwater are calculated by the three methods as described in Section 2.3. A comparison of the forces predicted by the three methods is given in Fig. 6 in time series, and the methods are indicated by acronyms. In general, the predictions of forces by the proposed model (IB and PI) are acceptable qualitatively. Forces during the wave run-up event agreed with the forces defined by GF. After reflection of a wave on the caisson wall, the force gradually reduced so that the wall experiences negative forces as if the wall is sucked into the offshore side. Although, the predictions by the LB methods have similar tendencies, the force in the PI method appears to underestimate the horizontal force and overestimates the lifting force, by contrast. More precisely, the sharp oscillations of the force after the third wave have been recorded in the time series of the lifting force by both approaches of the LBM in Fig. 6. We found that the oscillations were caused by the IB treatment for the seepage flow and they have no significant effects on the horizontal force estimation. It is possible to remove the effects of the IB on the pressure calculation for the seepage flow using a different approach or improving the IB solution as mentioned above. The current numerical model roughly estimates the pressure after the wave reflection on the caisson wall, and the estimation appears accurate when the next wave approaches the caisson wall, as shown in Fig. 6.

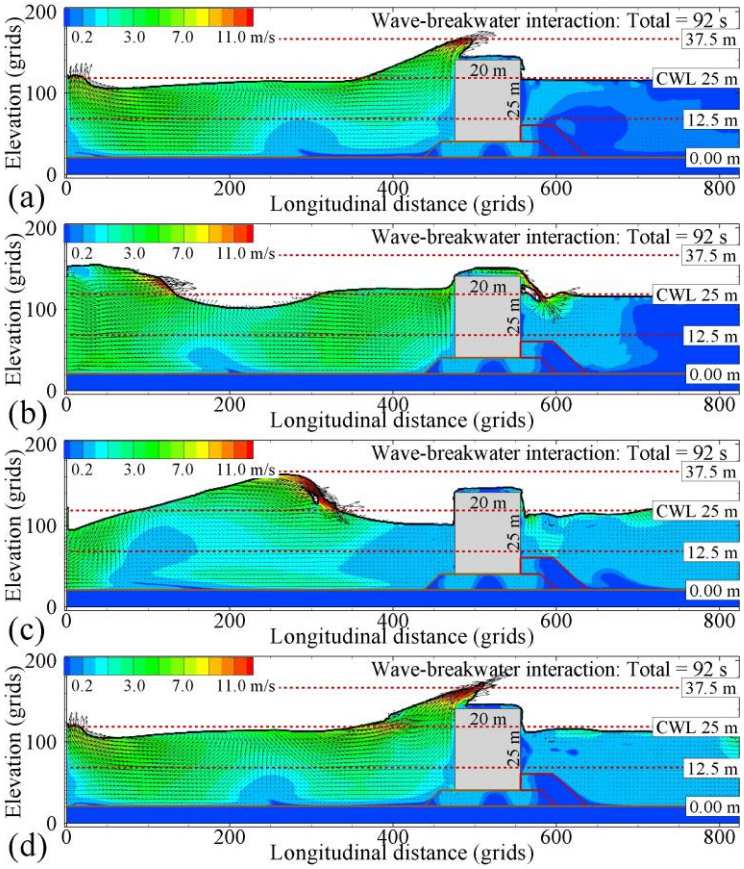

Figure 5. Wave–breakwater interactions at the same times presented in Fig. 3.

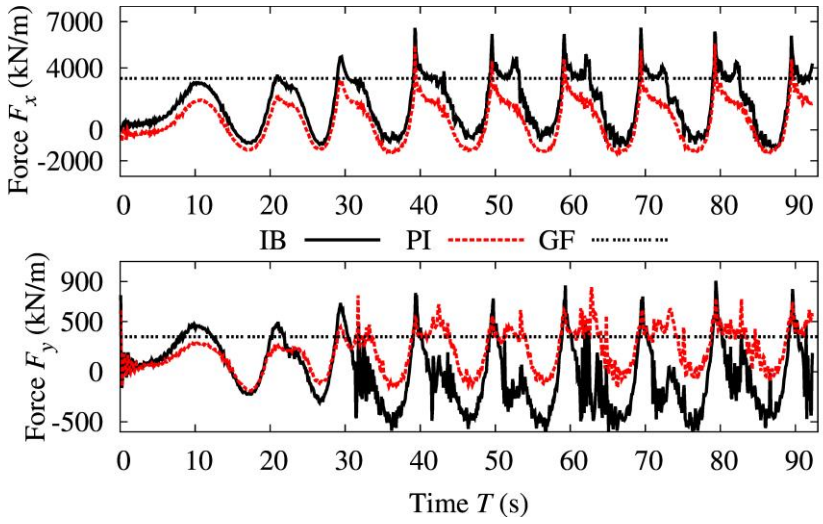

Figure 6. Force time series for the breakwater by three methods.

The horizontal distributions of the dynamic pressures acting on the caisson wall during the run-up event at two subsequent times are compared to Goda's pressure distribution in Fig. 7. The red dashed line shows the pressure distribution at the time when the wave crest touches the wall surface, whereas the dashed black line shows the pressure distribution at the time when the wave run-up and front plunges over the top of the caisson wall. The shape of the pressure distribution by the LBM forms into two triangular shapes facing each other with the highest value on the NWL as GF shows. A good agreement on the pressure distribution is found using the proposed model.

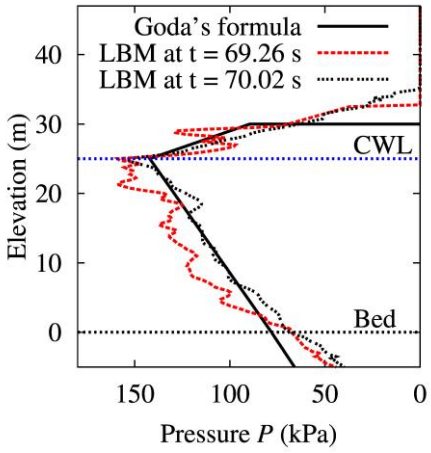

Figure 7. Pressure distribution at the caisson wall at two successive times during the run-up event.

4. Conclusions

Conclusively, wave forces acting on a typical breakwater representing other coastal structures are properly analyzed by the proposed model, and the predicted results were in good agreement with GF. The main features of this study are (1) the coupling of the free surface model with the IB method in the LB modeling and (2) the introduction of a simple, feasible, and compact LB model for wave force estimation and wave–structure interactions as an alternative novel numerical method. Comparing to the other competitive numerical models, such as SPH or MPS and VOF based on Reynolds-averaged Navier-Stokes equations, the FS-IB-LBM is rather cheap in computational time and has the same or better accuracy in results. In addition, the model is superior to the above models by providing the solutions for porous media flow under the breakwater and the motion of the immersed bodies without extending or modifying the model. To avoid unstable computations of very violent flows, the only disadvantage of the model, the FS-IB-LBM can be improved by using advanced fluid kinetic models.

5. References

Aidun, C. K., and Clausen, J. R. (2010). "Lattice-Boltzmann method for complex flows." *Annual review of fluid mechanics*, 42, 439-472.

Altomare, C., Crespo, A. J., Domínguez, J. M., Gómez-Gesteira, M., Suzuki, T., and Verwaest, T. (2015). "Applicability of Smoothed Particle Hydrodynamics for estimation of sea wave impact on coastal structures." *Coastal Engineering*, 96, 1-12.

Araki, T., and Koshimura, S. (2009). "Numerical Modeling of Free Surface Flow by the Lattice Boltzmann Method." *J.of JSCE, Ser. B2 (Coast. Eng.)*. 65 (1), 56-60.

Araki, T., and Koshimura, S. (2010). "Numerical Modeling of Multi-Phase (Water-Oil) Flow by Lattice Boltzmann Method." *J. of JSCE, Ser. B2 (Coast. Eng.)*, 66(1), 66-70.

Ayurzana, B., Khenmedekh, L., and Hosoyamada, T. (2017). "Parallel implementation of Entropic lattice Boltzmann method for flow past a circular cylinder at high Reynolds number." *Transactions on GIGAKU* 4(1), 04006/1-8

Badarch, A., Tokuzo, H., and Narantsogt, N. (2016). "Hydraulics application of the Free-surface Lattice Boltzmann method." *In Strategic Technology (IFOST), 2016 11th International Forum on*. IEEE, 195-199

Badarch, A. (2017). "Application of macro and mesoscopic numerical models to hydraulic problems with solid substances." PhD thesis, Nagaoka

Badarch, A., and Tokuzo, H. (2018). "Lattice Boltzmann method for the numerical simulations of the melting and floating of ice." *Free surface flows and transport processes*, Springer, Jachranka

Chen, S., and Doolen, G. D. (1998). "Lattice Boltzmann method for fluid flows." *Annual review of fluid mechanics*, 30(1), 329-364.

De Rosis, A., and Lévêque, E. (2016). “Central-moment lattice Boltzmann schemes with fixed and moving immersed boundaries.” *Computers & Mathematics with Applications*, 72(6), 1616-1628.

Dorschner, B., Chikatamarla, S. S., and Karlin, I. V. (2017). “Fluid-Structure Interaction with the Entropic Lattice Boltzmann Method.” *arXiv preprint arXiv: 1710.02375*.

Feng, Z. G., and Michaelides, E. E. (2004). “The immersed boundary-lattice Boltzmann method for solving fluid–particles interaction problems.” *Journal of Computational Physics*, 195(2), 602-628.

Goda, Y. (2010). Random seas and design of maritime structures, World scientific, Tokyo.

Guanche, R., Losada, I. J., and Lara, J. L. (2009). “Numerical analysis of wave loads for coastal structure stability.” *Coastal Engineering*, 56(5), 543-558.

Hayakawa, N., Hosoyamada, T., Yoshida, S. and Tsujimoto, G. (1998). “Numerical simulation of wave fields around the submerged breakwater with SOLA-SURF method.” *Coastal Engineering*, 843-852.

He, L. (2014). Modeling 3D Numerical Movable Bed based on LBM and its Application to the Analysis of Bed-Load Transport and Tsunami Drifts. PhD thesis, Nagoya.

Hou, S., Sterling, J., Chen S., Doolen GD. (1996). “A lattice Boltzmann subgrid model for high Reynolds number flows.” *Fields Inst. Comm.* 6:151-66

Janßen, C., and Krafczyk, M. (2011). “Free surface flow simulations on GPGPUs using the LBM.” *Computers & Mathematics with Applications*, 61(12), 3549-3563.

Körner, C., Thies, M., Hofmann, T., Thürey, N., and Rüde, U. (2005). “Lattice Boltzmann model for free surface flow for modeling foaming.” *Journal of Statistical Physics*, 121(1-2), 179-196.

Koshimura, S. and Murakami, K. (2009). “Application of the Lattice Boltzmann method for Tsunami modeling.” *J.of JSCE, Ser. B2 (Coast. Eng.)*. 65 (1), 256-260.

Noble, D. R., and Torczynski, J. R. (1998). “A lattice-Boltzmann method for partially saturated computational cells.” *International Journal of Modern Physics C*, 9(08), 1189-1201.

Strack, O. E., and Cook, B. K. (2007). “Three-dimensional immersed boundary conditions for moving solids in the lattice-Boltzmann method.” *International Journal for Numerical Methods in Fluids*, 55(2), 103-125.

Zhou, J. G. (2010). “A lattice Boltzmann model for the shallow water equations.” *Com. Meth. In App. Mech. And Eng*. 191(32), 3527-3539.

Zou, Q., He, X. (1997). “On pressure and velocity boundary conditions for the lattice Boltzmann BGK model.” *Phys. Fluids*. 9:1591-1598.